4-8-2013

Atomic force microscopy-coupled microcoils for cellular-scale nuclear magnetic resonance spectroscopy

Charilaos Mousoulis
Birck Nanotechnology Center, Purdue University, cmousoul@purdue.edu

Teimour Maleki
Birck Nanotechnology Center, Purdue University, tmalekij@purdue.edu

Babak Ziaie
Birck Nanotechnology Center, Purdue University, bziaie@purdue.edu

Corey Neu
Birck Nanotechnology Center, Purdue University, cpneu@purdue.edu

AIP | Applied Physics Letters

Atomic force microscopy-coupled microcoils for cellular-scale nuclear magnetic resonance spectroscopy

Charilaos Mousoulis, Teimour Maleki, Babak Ziaie, and Corey P. Neu

Citation: Appl. Phys. Lett. **102**, 143702 (2013); doi: 10.1063/1.4801318
View online: http://dx.doi.org/10.1063/1.4801318
View Table of Contents: http://apl.aip.org/resource/1/APPLAB/v102/i14
Published by the AIP Publishing LLC.

Atomic force microscopy-coupled microcoils for cellular-scale nuclear magnetic resonance spectroscopy

Charilaos Mousoulis,[1] Teimour Maleki,[2,a)] Babak Ziaie,[1,2,3] and Corey P. Neu[1,b)]
[1]*Weldon School of Biomedical Engineering, Purdue University, West Lafayette, Indiana 47907, USA*
[2]*Department of Electrical and Computer Engineering, Purdue University, West Lafayette, Indiana 47907, USA*
[3]*Birck Nanotechnology Center, Purdue University, West Lafayette, Indiana 47907*

(Received 6 February 2013; accepted 26 March 2013; published online 11 April 2013)

We present the coupling of atomic force microscopy (AFM) and nuclear magnetic resonance (NMR) technologies to enable topographical, mechanical, and chemical profiling of biological samples. Here, we fabricate and perform proof-of-concept testing of radiofrequency planar microcoils on commercial AFM cantilevers. The sensitive region of the coil was estimated to cover an approximate volume of $19.4 \times 10^3\ \mu m^3$ (19.4 pl). Functionality of the spectroscopic module of the prototype device is illustrated through the detection of ^1H resonance in deionized water. The acquired spectra depict combined NMR capability with AFM that may ultimately enable biophysical and biochemical studies at the single cell level. © *2013 AIP Publishing LLC* [http://dx.doi.org/10.1063/1.4801318]

Technologies that provide information on the single cell level may inevitably reveal specific mechanisms in a broad range of biological processes, from embryogenesis to aging. Most modern technologies study large populations of cells, with persistent heterogeneity in different stages of growth or disease, yielding only an average measure of cellular function. Studies at the single cell level are necessary to minimize variability of measures from cell populations, and enable detailed investigations for advanced cellular knowledge.[1]

Information extracted from such studies is particularly useful when correlated with cell mechanics and adhesion properties. There is a variety of techniques that can elucidate these properties, e.g., magnetic tweezers,[2,3] optical tweezers,[4] and atomic force microscopy (AFM).[5,6] A comprehensive review illustrating the strengths and weaknesses of these techniques applied to single molecules is given by Neuman and Nagy.[7] AFM provides a method of cellular stiffness measurement, in a non-destructive way by applying nanoscale forces. As opposed to the traditional optical imaging, AFM indirectly visualizes the cell surface morphology via monitoring the deflection of a sensing cantilever. AFM can further acquire stretching curves, through the pressing of the cantilever on the surface and determine the subsequent stiction during the tip retraction. A distinct advantage of this technology is that other techniques such as brightfield,[8] confocal,[9] and fluorescence[10] microscopy can be incorporated to enable detection of cellular shape and labeling of proteins on the cell interior.

We developed a technology to further improve the biochemical profiling attained on AFM-based platforms, by incorporating a planar micro-coil on top of the AFM cantilever that is designed to enable NMR signal acquisition in addition to topographical and biophysical profiling. This technology potentially exhibits numerous advantages: First, it enables studies of heterogeneity between cells of similar phenotype, which, in cases such as cancer, can provide valuable mechanistic insight which may lead to more effective treatments.[11] Second, it facilitates identification and classification of malignant cells, thanks to the NMR functionality[12–14] (e.g., through the study of the metabolic phenotype). Third, NMR can provide insightful intercellular chemical information while the mechanical interaction of the cell with the matrix is studied by AFM; matrix stiffness has been shown to influence proliferation and tumorigenesis;[15] therefore, the conjunction of the NMR technology can provide insights to guide the development of therapies.

The prototype device presented in this Letter is the basic element of a technology for the selective cell analysis through the integration of planar NMR microcoils with AFM probes to obtain a hybrid probe that is designed to operate in conventional high-frequency (e.g., 500 MHz) NMR magnets. The outcomes of our AFM-coupled microcoil (hereafter termed AFM/NMR probe) may include, but are not limited to, the nanoscale spatial localization, as well as the biophysical and physicochemical analysis features of AFM combined with the spectroscopic capabilities of NMR for the real-time microscopy and structural analysis of single cells.

Our objective is to demonstrate the spectroscopic feature of the hybrid AFM/NMR probe. Establishment of the operational NMR function of the probe is the feasibility cornerstone of the presented technology, and is of particular significance, because it demonstrates the ability to add the NMR function to commercially available AFM probes with minor modifications. This technology can also be coupled with chemically functionalized AFM probes for the investigation of specific unbinding forces.

A hybrid AFM/NMR probe contains basic elements for combined sensing, including the radiofrequency (RF) coil (Figure 1). The coil serves both as the transmitter and receiver of the RF pulses. The planar NMR coil is formed by nanofabrication techniques on the top of the cantilever beam of the AFM probe. The connections to the tuning/matching circuitry of the NMR system are through gold contact pads located on the anchor of the cantilever beam. The attained NMR spatial resolution is in the micrometer range since the inner diameter of the coil is less than 100 μm. The deflection of the beam

a)Present address: Bruker Nano Surfaces Division, Santa Barbara, CA 93117.
b)Author to whom correspondence should be addressed. E-mail: cpneu@purdue.edu. Tel: (765) 496-1426. Fax: (765) 494-0902.

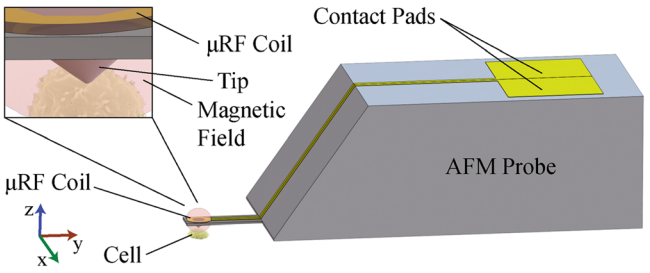

FIG. 1. A hybrid AFM/NMR probe technology combined AFM-coupled microcoils for NMR signal detection at the cellular scale. A commercial AFM probe was modified using nanotechnology fabrication processes to include a radiofrequency microcoil over the tip of the cantilever. Operation of the hybrid probe will include contact with the cell under investigation (using piezoelectric or other sensing feedback mechanisms) for combined biophysical (AFM) and biochemical (NMR) measurements.

when the tip is brought in contact with the cell can be monitored through a typical laser system, interferometry, or by the addition of a piezo-electric layer to the cantilever. Following contact, the force-displacement curve can be obtained. Adhesion force is measured as the pull-off force upon tip separation from the surface during unloading.

The proof-of-concept was demonstrated by fabricating a prototype AFM/NMR probe (Figure 2). A commercially available AFM silicon probe (Tap-Tall, Applied NanoStructures Inc., Mountain View CA) was used to fabricate the device. Initially, a 100 nm thin layer of Parylene-C (Specialty Coating Systems, Indianapolis, IN) was uniformly deposited (Figure 2(a)) in order to provide the electrical insulation between the silicon and subsequent gold microcoil, thus eliminating parasitic effects and current leakage. A 1.5 μm thick layer of Au was then deposited on the entire top surface of the probe through RF plasma sputtering. Subsequently, focused ion beam (FIB) milling (FEI Nova 200 Nanolab) was performed to define the planar coil. An octagonal-shaped coil was patterned with inner radius of 24 μm on the longitudinal and 16 μm on the transverse direction of the cantilever (Figure 2(b)). The

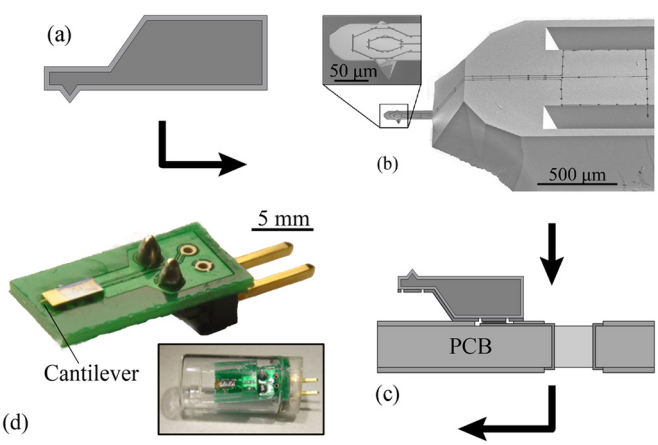

FIG. 2. AFM/NMR probe fabrication and assembly involved standard processing of commercially available AFM cantilevers. The probe fabrication process involved multiple steps: (a) a commercial AFM silicon cantilever was covered uniformly with 100 nm Parylene-C for electrical insulation; (b) gold was deposited with plasma sputtering and focused ion beam etching was performed for the definition of the NMR coil and connection pad geometry; (c) the probe was bonded to the custom-designed board through manual flip-chip alignment and bonding; (d) following epoxy underfill for securing the bond, the electrical connection was soldered, and the device was packaged in a glass vial for the insertion and the removal of the liquid samples (inset).

average width of the coil was 26.71 μm. By using the FIB patterning method, manufacturing yield was attained, and the induced stress on the cantilever did not lead to undesired deflection and bending. The device was flip-chip bonded to a custom-designed printed circuit board (PCB) using a conductive adhesive (118-09 A/B-187, Creative Materials Inc., Tyngsboro, MA) (Figure 2(c)). Finally, the bond was secured with an epoxy, and the connector was soldered on the PCB (Figure 2(d)). The device was then encapsulated in a glass vial, sealed with a silicone cap for the easy injection of liquid samples (Figure 2(d), inset) for subsequent NMR studies.

In order to estimate the performance of the AFM/NMR probe's microcoil, a finite element analysis (FEA) was performed using HFSS (Ansys Inc.) (Figure 3). The magnitude of the magnetic flux density, $B_{1,xz}(\vec{r}) = \sqrt{B_{1,x}^2(\vec{r}) + B_{1,z}^2(\vec{r})}$, on the plane xz perpendicular to the direction y of the magnet's field B_o was calculated. The acquired values represent the resulting field due to the input of 6.29 W at the connection pads of the coil. The amplitude of the simulation input corresponds to the amplifier power used in NMR experiments described below. The inductance and resistance of the coil given by the finite element analysis were 0.86 nH and 3.27 Ω, respectively. The measured resistance of the whole device (i.e., coil mounted on the PCB) was 7.23 Ω.

An estimate of the excitation volume of the AFM/NMR probe microcoil was acquired using the experimental value of the applied power to the probe and the FEA model. The excitation volume was considered herein equal to the "sensitive region" of the surface coil,[16] i.e., the sample volume that senses the on-resonance RF signal induced by the coil (during transmission) and provides a readable free induction decay (during reception). In the case of a circular coil of radius a, this region is enclosed within the boundaries $z \leq \frac{a}{2}, x \leq a$, where z is the axis normal to the coil plane, and x is the axis on the coil plane parallel to the static magnetic field. In this case, however, where the inner area of the coil is assumed to be an ellipse, the sensitive region can be approximated by the volume given by the ellipse area times half the radius of the minor axis. Therefore, theoretically, the threshold sensing distance is 8 μm, which is adequate for in-cell NMR measurements, and the overall sensitive region on each side of the surface coil is $9.7 \times 10^3\ \mu m^3$ (or 9.7 pl). Assuming an average diameter of 20 μm for mammalian

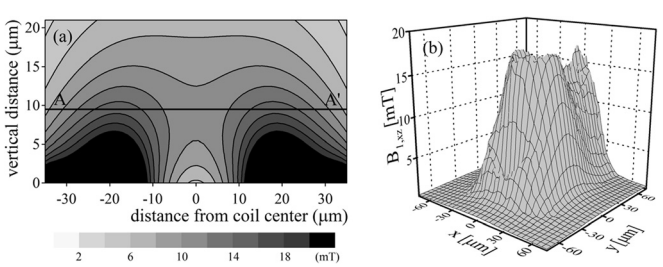

FIG. 3. The transmission performance of the AFM/NMR probe was estimated using finite element analysis. Magnetic flux density due to the RF coil varied spatially on the plane through the center of the coil and perpendicular to the static magnetic field (a). Section AA′ indicates the vertical limit of the sensitive region of the coil as determined based on the coil radius; (b) magnitude of the field at the plane parallel to the coil at distance indicated by AA′. The axis of the static magnetic field is along y.

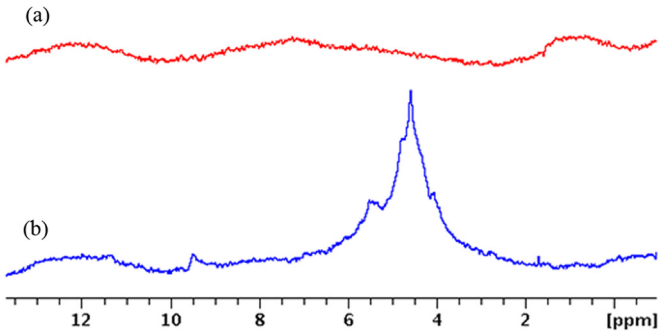

FIG. 4. The AFM/NMR probe detection of NMR signals was demonstrated using (a) deuterium oxide (control) and (b) de-ionized water. The baseline of the spectra is not flat throughout the whole frequency range due to the contribution of the Parylene-C insulation layer. An internal reference signal was not used in this set of experiments.

cells, and a volume of $33.5 \times 10^3\ \mu m^3$, the fabricated microcoil is capable of in-cell NMR signal detection.

To demonstrate our ability to acquire NMR spectra with our hybrid AFM/NMR probe technology as a proof-of-concept, the fabricated microcoil was configured for signal detection of common liquids. For the experimental measurements, the assembly was mounted on a custom fixture developed for the *in situ* tuning/matching before and after the insertion in the magnet.[17] A series capacitive matching circuit[16] was used with tunable capacitors. The capacitance values were 53 pF and 4 pF for the tuning and the matching capacitors, respectively. The inductance element of the matching circuit consisted of a 5-turn coil positioned parallel to the tuning capacitor. A 500 MHz Bruker NMR spectrometer (Bruker DRX500) was used to evaluate the performance of the probe. Two liquids were employed as phantom materials for the detection of probe functionality: deuterium oxide and de-ionized water. A pulse-acquire program was used for the spin excitation and signal acquisition (zg pulse sequence, TopSpin 1.3). Data were acquired using a 5 μs pulse length with an acquisition time of 0.22 s, recycle delay of 0.20 s, and 16 accumulations.

The hybrid AFM/NMR probe successfully detected spectra from liquid phantom materials (Figure 4). Deuterium oxide was used as the negative control sample for the device and did not produce a chemical shift spectrum, as expected, due to the lack of ^1H protons in the sample. However, the probe detected successfully the de-ionized H_2O sample (Figure 4(b)). Interestingly, the demonstrated proof-of-concept NMR functionality of the commercial AFM probe suffered from a small number of anomalies that were noted on the observed spectra. First, the baselines were not flat throughout the whole frequency range, which was attributed to the broad background peaks due to the use of Parylene-C for the electrical insulation. Future device implementations will employ silicon nitride probes in order to eliminate the need for this insulation barrier. Second, the prototype device provided relatively broad resonance signal with low SNR, due to the inhomogeneous field distribution caused primarily by the layout and materials used in the commercially available AFM cantilever assembly. Since these performance issues were inherent due to the limited microfabrication processes that can be applied on released cantilevers, our current focus is on the development of AFM cantilevers with embedded NMR functionality, in order to attain high quality NMR detection on cantilevers specifically designed for cell interaction. In this way, it can be ensured that the devices will satisfy the critical design parameters, e.g., low spring constant, well-defined impedance, increased quality factor ($\boldsymbol{Q}$) due to lower dc resistance, and improved field homogeneity that will facilitate the synchronous AFM and NMR operation.

In conclusion, we demonstrated the successful resonance spectroscopy operation of a hybrid AFM/NMR probe. The prototype was built using a commercially available AFM cantilever, and provided distinctive spectra for a variety of samples operating in a transmit/receive mode inside a standard NMR system. The complementary feature of AFM for concurrent biophysical measurements, beyond the scope of the present work, is currently being investigated. The significance of our hybrid AFM/NMR probe technology is eminent, since in the long term it is expected to facilitate the understanding of combined biophysical (e.g., mechanical stiffness) and biochemical (e.g., metabolic) processes within single cells to provide fundamental biomedical information, and insight for the development of therapies.

The authors gratefully acknowledge financial support from the Showalter Trust Fund and NIH R21 AR064178. The authors also thank Dr. Daniel Raftery for the usage of his probe fixture, Dr. John Harwood for his assistance in the spectroscopy acquisitions, and Dr. David Reiter for his helpful manuscript comments.

[1]S. Altschuler and L. Wu, Cell **141**(4), 559 (2010).
[2]A. Bausch, W. Moller, and E. Sackmann, Biophys. J. **76**(1), 573 (1999).
[3]C. Gosse and V. Croquette, Biophys. J. **82**(6), 3314 (2002).
[4]F. Wottawah, S. Schinkinger, B. Lincoln, R. Ananthakrishnan, M. Romeyke, J. Guck, and J. Kas, Phys. Rev. Lett. **94**(9), 098103 (2005).
[5]G. Binnig, C. Quate, and C. Gerber, Phys. Rev. Lett. **56**(9), 930 (1986).
[6]A. Raman, S. Trigueros, A. Cartagena, A. Stevenson, M. Susilo, E. Nauman, and S. Contera, Nature Nanotechnol. **6**(12), 809 (2011).
[7]K. Neuman and A. Nagy, Nature Meth. **5**(6), 491 (2008).
[8]E. Canetta, A. Duperray, A. Leyrat, and C. Verdier, Biorheology **42**(5), 321 (2005).
[9]G. Charras and M. Horton, Biophys. J. **82**(6), 2970 (2002).
[10]O. Chaudhuri, S. Parekh, W. Lam, and D. Fletcher, Nature Meth. **6**(5), 383 (2009).
[11]M. Shackleton, E. Quintana, E. Fearon, and S. Morrison, Cell **138**(5), 822 (2009).
[12]F. Lehnhardt, C. Bock, G. Rohn, R. Ernestus, and M. Hoehn, NMR Biomed. **18**(6), 371 (2005).
[13]C. Florian, N. Preece, K. Bhakoo, S. Williams, and M. Noble, Cancer Res. **55**(2), 420 (1995).
[14]J. Griffin and J. Shockcor, Nature Rev. Cancer **4**(7), 551 (2004).
[15]M. Paszek, N. Zahir, K. Johnson, J. Lakins, G. Rozenberg, A. Gefen, C. Reinhart-King, S. Margulies, M. Dembo, D. Boettiger, D. Hammer, and V. Weaver, Cancer Cell **8**(3), 241 (2005).
[16]J. Mispelter, M. Lupu, and A. Briquet, *NMR Probeheads for Biophysical and Biomedical Experiments: Theoretical Principles & Practical Guidelines* (Imperial College Press, London, UK, 2006).
[17]R. Kc, I. Henry, G. Park, and D. Raftery, J. Magn. Reson. **197**(2), 186 (2009).